Available online at www.sciencedirect.com
ScienceDirect
Cellular Signalling 19 (2007) 2612–2624
CELLULAR SIGNALLING
www.elsevier.com/locate/cellsig

^{1}H NMR structural and functional characterisation of a cAMP-specific phosphodiesterase-4D5 (PDE4D5) N-terminal region peptide that disrupts PDE4D5 interaction with the signalling scaffold proteins, βarrestin and RACK1

K. John Smith [b,1,2], George S. Baillie [a,1], Eva I. Hyde [b], Xiang Li [a], Thomas M. Houslay [a,3], Angela McCahill [a], Allan J. Dunlop [a], Graeme B. Bolger [e], Enno Klussmann [c], David R. Adams [d], Miles D. Houslay [a,*]

[a] *Molecular Pharmacology Group, Division of Biochemistry & Molecular Biology, Wolfson Link Building, IBLS, University of Glasgow, Glasgow G12 8QQ, Scotland, UK*
[b] *School of Biosciences, University of Birmingham, Edgbaston, Birmingham, PO Box 363, B15 2TT, UK*
[c] *Leibniz-Institut für Molekulare Pharmakologie (FMP), Campus Berlin-Buch, Robert-Rössle-Str. 10, 13125 Berlin, Germany*
[d] *Department of Chemistry, Heriot-Watt University, Riccarton Campus, Edinburgh, EH14 4AS, Scotland, UK*
[e] *University of Alabama at Birmingham, Comprehensive Cancer Center, Birmingham, Alabama 35294-3300, USA*

Received 21 August 2007; accepted 26 August 2007
Available online 1 September 2007

Abstract

The unique 88 amino acid N-terminal region of cAMP-specific phosphodiesterase-4D5 (PDE4D5) contains overlapping binding sites conferring interaction with the signaling scaffold proteins, βarrestin and RACK1. A 38-mer peptide, whose sequence reflected residues 12 through 49 of PDE4D5, encompasses the entire N-terminal *RA*CK1 *I*nteraction *D*omain (RAID1) together with a portion of the βarrestin binding site. ^{1}H NMR and CD analyses indicate that this region has propensity to form a helical structure. The leucine-rich hydrophobic grouping essential for RACK1 interaction forms a discrete hydrophobic ridge located along a single face of an amphipathic α-helix with Arg34 and Asn36, which also play important roles in RACK1 binding. The Asn22/Pro23/Trp24/Asn26 grouping, essential for RACK1 interaction, was located at the N-terminal head of the amphipathic helix that contained the hydrophobic ridge. RAID1 is thus provided by a distinct amphipathic helical structure. We suggest that the binding of PDE4D5 to the WD-repeat protein, RACK1, may occur in a manner akin to the helix–helix interaction shown for G_{γ} binding to the WD-repeat protein, G_{β}. A more extensive section of the PDE4D5 N-terminal sequence (Thr11-Ala85) is involved in βarrestin binding. Several residues within the RAID1 helix contribute to this interaction however. We show here that these residues form a focused band around the centre of the RAID1 helix, generating a hydrophobic patch (from Leu29, Val30 and Leu33) flanked by polar/charged residues (Asn26, Glu27, Asp28, Arg34). The interaction with βarrestin exploits a greater circumference on the RAID1 helix, and involves two residues (Glu27, Asp28) that do not contribute to RACK1 binding. In contrast, the interaction of RACK1 with RAID1 is extended over a greater length of the helix and includes Leu37/Leu38, which do not contribute to βarrestin binding. A membrane-permeable, stearoylated Val12-Ser49 38-mer peptide disrupted the interaction of both βarrestin and RACK1 with endogenous PDE4D5 in HEKB2 cells, whilst a cognate peptide with a Glu27Ala substitution selectively failed to disrupt PDE4D5/RACK1 interaction. The stearoylated Val12-Ser49 38-mer peptide enhanced the isoprenaline-

Abbreviations: GST, glutathione S-transferase; PDE4, cyclic AMP specific phosphodiesterase family 4; PDE4D5, PDE4 sub-family D isoform 5; RAID1, *RA*CK1 *I*nteraction *D*omain; cAMP, cyclic 3′,5′-adenosine monophosphate; β_2-adrenergic receptors (β_2AR); COSY, ^{1}H–^{1}H correlated spectroscopy; NOE, nuclear Overhauser effect/enhancement; NOESY, nuclear Overhauser effect spectroscopy; TOCSY, total correlated spectroscopy.

* Corresponding author. Tel.: +44 141 330 5903; fax: +44 141 330 4365.
E-mail address: M.Houslay@bio.gla.ac.uk (M.D. Houslay).

[1] To be considered as joint first authors.
[2] Current address: Department of Biophysics, Biochemistry and Chemistry, University of Michigan, Ann Arbor, MI, USA.
[3] Current address: AstraZeneca, Loughborough, UK.

doi:10.1016/j.cellsig.2007.08.015

stimulated PKA phosphorylation of the β_2-adrenergic receptors (β_2AR) and its activation of ERK, whilst the Glu27Ala peptide was ineffective in both these regards.

Keywords: Rolipram; RACK1; βarrestin; NMR structure; Signalling scaffold; Cyclic AMP; Protein–protein interaction; Peptide displacement; Spot immobilised peptide arrays; β_2-adrenergic receptors (β_2AR); ERK; PKA

1. Introduction

cAMP is a ubiquitous second messenger that regulates numerous key physiological processes [1–4]. Its levels are determined both by controls on its rate of synthesis through adenylyl cyclase activity and its rate of degradation through cAMP phosphodiesterase (PDE) activity [5]. A large multigene family encodes many proteins that exhibit PDE activity [6]. Of these, the PDE4 cAMP-specific phosphodiesterases have attracted considerable attention as inhibitors that are selective for them have behavioural, anti-inflammatory and smooth-muscle relaxant activity in humans [7–12]. They can be differentiated from other cyclic nucleotide phosphodiesterase families on the basis of sequence differences in their catalytic region and by their ability to be specifically inhibited by the drug, rolipram [7,8,13,14]. Mammalian PDE4s comprise a large family of isoforms, encoded by four different genes (*PDE4A*, *PDE4B*, *PDE4C*, and *PDE4D*) [7,8], with additional diversity being generated by alternative mRNA splicing and the use of alternative promoters [15–19]. A characteristic feature of these different isoforms is their unique N-terminal regions. Subsequent to the archetypal studies performed on PDE4A1 [20–24], these isoform-specific N-terminal regions have been shown to play a key role in the targeting of various PDE4 isoforms to specific signalling complexes and intracellular sites [8,9,25–27]. In this way PDE4 isoforms perform a major role in underpinning compartmentalized cAMP signalling in many cell types [28–34]. The PDE4 enzymes are also characterised by unique regulatory regions located in the amino-terminal half of the proteins, called Upstream Conserved Regions 1 and 2 (UCR1 and UCR2) [35]. Both UCR1 and UCR2 appear to interact with each other in order to form a regulatory module that mediates the functional outcome of phosphorylation by PKA and ERK [36–38].

PDE4D5 is one of the nine different isoforms encoded by the *PDE4D* gene and is found in a variety of tissues and cell types, including the brain [39]. PDE4D5 is distinguished from other PDE4D isoforms by the presence of a unique amino-terminal region of 88 amino acids, which is highly conserved among mammals. We have demonstrated that PDE4D5 can interact directly with the signalling scaffold proteins, RACK1 and βarrestin in two-hybrid screens, pull-down assays and in both peptide array and phage-presenting peptide screens [40–44]. Using a novel scanning peptide array methodology coupled to mutagenesis in both pull-down and 2-hybrid studies we have shown that RACK1 and βarrestin bind to overlapping sites within the isoform-specific N-terminal region of PDE4D5 as well as to discrete, abutting sites within the common PDE4 catalytic unit [40]. It is the presence of these additional sites within its unique N-terminal region that allows endogenously expressed PDE4D5 to interact specifically with RACK1 and preferentially with βarrestin in cells [40,45].

RACK1 is a 36-kDa WD-repeat protein [42] that was first identified [46] as a protein that could bind to certain protein kinase C (PKC) isoforms subsequent to their activation by either diacylglycerol or phorbol esters. However, RACK1 is now known to interact with a variety of proteins including the b-subunit of integrins, the common beta-chain of the IL-5/IL-3/GM-CSF receptor, SRC tyrosyl protein kinase, the type II bone morphogenetic protein receptor (BMPRII), NHERF1, HIF1α, β-spectrin and dynamin, for example [42,47–54]. In doing this RACK1 acts as a scaffold to bring together proteins that effect and regulate a variety of important cellular processes. Notwithstanding this, little is known about the functional consequences of PDE4D5 interaction with RACK1 and thus reagents are required that allow for the specific disruption of this complex in order to gain functional insight.

βarrestin is now considered to act as a scaffold protein that regulates a number of important cellular processes [55–57]. However, it is most well-known for its role in effecting the desensitization of G-protein coupled receptors. For example, β_2-adrenergic receptors (β_2AR) couple to the G-protein G_s in an agonist-dependent fashion so as to activate adenylyl cyclase and thereby increase intracellular cAMP levels. This response becomes rapidly desensitized when the agonist-occupied β_2AR becomes phosphorylated by the G-protein receptor coupled kinase, GRK2. This triggers the recruitment of βarrestins from the cytosol, which then sterically interdict coupling of the β_2AR with G_s. Recently, a new feature of this desensitization system has been identified, namely that βarrestin-sequestered PDE4D5 can be delivered to the β_2AR in an agonist-dependent fashion [26,27,40,45,58–61]. This increases cAMP degradation in the locality of the β_2AR, which attenuates the functioning of a discrete pool of cAMP-dependent protein kinase (PKA) tethered to the β_2AR by AKAP79 [45]. One action of βarrestin-sequestered PDE4D5, on recruitment to the β_2AR, is thus to attenuate the phosphorylation of the β_2AR by PKA. In certain cells, such as cardiac myocytes, the PKA-mediated phosphorylation of the β_2AR allows it now to couple G_i and thereby effect the activation of ERK in a src-dependent fashion [26,27,62]. In cells such as cardiac myocytes this generates a functional correlate as βarrestin recruited PDE4, in diminishing the phosphorylation of the β_2AR by PKA, attenuates the ability of the β_2AR to couple to G_i and activate ERK.

Although PDE4 enzymes as a family can be selectively inhibited [10,11,63], the identical catalytic units exhibited within a particular sub-family, together with close homology between sub-families, precludes using active site directed inhibitors either as tools for understanding the functional role of isoforms or as

isoform specific therapeutics. Over the years we have developed the notion that reagents able to displace specific isoforms from specific signalling complexes in cells could provide isoform specific 'inhibitors', with our development of catalytically inactive PDE4 isoforms that display a dominant negative providing a functional paradigm [25,45,58]. We develop here cell-permeable peptide reagents based upon the N-terminal region of PDE4D5 that allow for the selective disruption of PDE4D5 targeting to specific signalling scaffolds, namely βarrestin and RACK1. These enable us to identify βarrestin-sequestered PDE4D5 as playing a unique role in regulating the isoprenaline-stimulated phosphorylation of the β_2AR by PKA and in the switching of its action to the activation of ERK. Using CD and ^{1}H NMR analyses we show that such a peptide has a propensity to form a helical structure that presents amino acids key to interaction with these scaffolds.

2. Materials and methods

2.1. Materials

Polyclonal antisera specific to the PDE4D sub-family were used as described previously [39,59]. An IgM monoclonal antibody against RACK1 was from BD Biosciences (San Jose, CA, USA). Antisera detecting βarrestin1/2 were from Dr R. Lefkowitz (Duke Univ., NC). Antibodies for detection of the native and phosphorylated forms of ERK1/2 and for detection of phosphoserine PKA substrates were from Cell Signaling Technologies (Beverley, MA, USA). Rabbit polyclonal antibody against the β_2AR and PKA P-β_2AR ser345/346 were from Santa Cruz Biotechnology (Santa Cruz, CA, USA). Protein A beads and IgM agarose were from Sigma-Aldrich (Poole, Dorset, UK). Protein A beads used in immunoprecipitation reactions were from Invitrogen (Paisley, Scotland, UK).

2.2. NMR

We have previously determined the structure of the unique N-terminal region of PDE4A1 using ^{1}H NMR spectroscopy [24]. In this study, analyses were done on a 38-mer peptide whose sequence (12VPEVDNPHCPNPWLNEDLVKSL-RENLLQHEKSKTARKS49) was contained within the unique N-terminal region of PDE4D5 [39,40,44,59]. ^{1}H NMR experiments were carried out on Bruker AMX500 and Varian UnityPlus600 spectrometers using standard phase sensitive two-dimensional pulse sequences. Two-dimensional experiments were acquired with 2048 or 4096 data points in the direct dimension F2, using a sweep width of between 9 and 12 ppm, and with up to 448 rows in the indirect dimension F1. For TOCSY and COSY experiments 32 transients were acquired, and for NOESY experiments up to 128 transients were acquired. TOCSY experiments used an MLEV-17 mixing pulse of 60-ms duration (10 kHz spin locking field). The NOESY experiments were collected with mixing times of 50, 100 and 200 ms. Very weak presaturation was applied to the water resonance both during the relaxation delay (1.5 s) and during the mixing time of the NOESY experiments. TOCSY, NOESY and COSY spectra for assignment were collected on 2.5 mM solutions of peptide in the presence of 2-fold molar excess of dithiothreitol, at pH 5.8 in 50% D_3-TFE/50% H_2O (v/v), at 293 K and 297 K. The addition of dithiothreitol eliminated the formation of intermolecular disulfide bridges. The chemical shifts were determined in TOCSY spectra at temperatures between 285 and 297 K. Temperature shift coefficients were determined from the slope of a linear plot of temperature against chemical shift. Inter-proton distances were estimated from NOESY experiments by integration of cross-peak volumes in the 200-ms NOESY spectrum (all cross-peaks were also seen at 100 ms of mixing time). Cross-peaks were grouped into five classes between strong and very weak (strong and medium NOEs were allocated the same distance constraint values in calculations). A small number of NOEs were defined by ambiguous constraints. Analysis of early calculated structures identified a number of short inter-proton distances that had no corresponding cross-peaks in the NOESY spectra. These were allocated weak repulsive restraints in order to exclude these short contacts. The peptide structure was determined using XPLOR 3.581 with ARIA extensions [64,65] using a protocol in which certain atoms of each residue were embedded using the distance geometry routine (atoms CA, HA, N, HN, C, CB*, CG*, dg_sub_embed protocol). The remaining atoms were placed by template fitting, and the atomic co-ordinates were allowed to evolve under the applied NOE distance constraints during a series of high temperature simulated annealing steps (dgsa and refine protocols). From the 100 calculated co-ordinate sets started, half were discarded (wrong handedness in the distance geometry routine). The final structures were produced by minimizing the averaged co-ordinates produced over the last 4 ps of a 5-ps low temperature simulated annealing trajectory. Twenty-five structures with no violations of the applied NOE constraints greater than 0.5 Å were then chosen for analysis. To aid analysis, a mean structure was calculated by simultaneously refining these 25 structures in a high temperature simulated annealing protocol and applying an additional constraint (NCS) tending to minimize the RMS difference between the aligned co-ordinates. Hydrogen bond constraints were included in calculations at a late stage, after NOE constraints had identified the position of hydrogen bonds. The pattern of hydrogen bond donors, indicated by changes in the rate of change in chemical shift of the backbone amides with changes in temperature, was consistent with the calculated structures. There were no significant differences between the NOEs observed at 293 and 297 K nor between NOEs observed with either 2.5 mM peptide or 0.6 mM peptide.

The PDB ID code for the co-ordinate entry is 1e9k and the NMR restraints entry is r1e9kmr for the peptide studied.

2.3. Circular dichroism (CD) analysis

CD spectra were measured between 190 nm and 300 nm on a JASCO 810 spectropolarimeter at 25 °C in either 10 mM Na_2HPO_4 buffer, pH 5.8, or 50% buffer, 50% trifluoroethanol (TFE). Samples of 200 μM in peptide were used in a 0.1-cm pathlength cuvette. The concentrations of the peptides were determined from the absorbance at 230 nm, using a molar absorbance of 300 M^{-1} cm^{-1} for each peptide bond. The percent alpha helicity was determined from the mean residue ellipticity at 222 nm, using a value of 30,000 for 100% alpha helix [66].

2.4. SPOT synthesis of peptides and overlay experiments

Peptide libraries were produced by automatic SPOT synthesis [67,68]. They were synthesized on continuous cellulose membrane supports on Whatman 50 cellulose membranes using Fmoc-chemistry with the AutoSpot-Robot ASS 222 (Intavis Bioanalytical Instruments AG, Köln, Germany). Interaction of peptide spots with MBP- or GST-fused purified proteins was determined as described by us previously [40,61] by overlaying the cellulose membranes with 10 μg/ml of recombinant protein. Bound recombinant proteins were detected with specific primary antisera and complementary HRP-coupled secondary antibody as for immunoblotting.

2.5. Cell culture

HEK293B2 cells were cultured as before [40,58,60,69]. They were maintained in Dulbecco's modified Eagle medium containing 10% fetal bovine serum with 1× penicillin/streptomycin. Cells were treated with isoprenaline (10 μM) for 5 min, as indicated. Immunopurification of RACK1 and βarrestin was done using endogenously expressed proteins.

2.6. Treatment with cell-permeable peptides

HEKB2 cells were treated with the indicated peptides (10 μM) for 2 h prior to stimulation with isoprenaline. Peptides were dissolved in DMSO at a stock concentration of 10 mM and added 1:1000v/v with cell culture medium. Control cells were treated with vehicle alone *i.e.* 0.1% DMSO.

2.7. SDS polyacrylamide gel electrophoresis and immunoblotting

These were as described previously. In brief, samples were resuspended in Laemmli buffer and boiled for 5 min. Membranes were blocked in 5% (w/v) low-fat milk powder in TBS (10 mM Tris–HCl, pH 7.4, 150 mM NaCl)

overnight at room temperature. They were then incubated with anti-VSV monoclonal antibody diluted in 1:5000 (v/v) in 1% (v/v) low-fat milk powder in TTBS (TBS plus 0.1% (v/v) Tween 20) for 3 h at room temperature. Detection of the bound antibody was with anti-mouse IgG peroxidase (Sigma) and the enhanced chemiluminescence (ECL) system (Amersham).

2.8. Immunopurification of βarrestin

Briefly, detergent-soluble proteins were isolated from cells by disruption in lysis buffer (1% (v/v) Triton X-100, 50 mM HEPES buffer, pH 7.2, 10 mM EDTA, 100 mM NaH_2PO_4) containing Complete (Roche) protease inhibitor mixture to 8% volume. Detergent-insoluble proteins were removed by centrifugation at 10,000 $\times g_{av}$ for 10 min, and the soluble fraction was retained. Equal volumes of cell lysate containing 500 μg of protein were cleared by incubation with 30 μl of protein A slurry. The beads were then removed by centrifugation at 10,000 $\times g_{av}$ for 10 min at 4 °C, and cleared lysate was incubated at 4 °C for 2 h with constant agitation with a volume of antiserum determined to immunoprecipitate βarrestin from the cells. Immunoglobulins were then isolated by incubation with protein-A-coated Sepharose beads for 1 h before retrieval by refrigerated centrifugation at 10,000 $\times g_{av}$ for 5 min. A similar protocol was used to isolate RACK1. Immunopurified proteins were run on SDS PAGE and immunoblotted.

2.9. Measurement of protein concentrations

Protein concentrations were measured by the method of Bradford [70], using BSA as a standard.

3. Results

Long PDE4 isoforms are characterised by the presence of two blocks of sequence, called UCR1 and UCR2, located between the conserved catalytic unit and the extreme N-terminal region that is unique to each isoform (Fig. 1). The unique amino-terminal region of PDE4D5 (Fig. 1) consists of a block of 88 amino acids that has no homology with any other PDE4 isoform. We have demonstrated previously that this region of PDE4D5 contains overlapping binding sites that allow it to bind, in a mutually exclusive fashion, to the signaling scaffold proteins βarrestin and RACK1 [40,44,45,59]. The conserved PDE4 catalytic unit also possesses adjacent binding sites for βarrestin and RACK1, allowing these scaffold proteins each to straddle separately PDE4D5 [40]. The PDE4 catalytic unit-located site for βarrestin allows all isoforms to interact with it, albeit much more weakly than PDE4D5. However, the PDE4 catalytic unit-located site for RACK1 is insufficient to allow other PDE4 isoforms to interact with it discernibly in cells. Thus a combination of N-terminal binding sites plus catalytic unit binding sites confers the unique ability for PDE4D5 to interact with RACK1 and a preference for βarrestin to interact with this isoform in cells [40]. However, the interaction of PDE4D5 with these scaffold proteins is mutually exclusive due to the overlap in the location of their binding sites within the enzyme's isoform-specific N-terminal region.

The RACK1-interacting domain within the N-terminal region of PDE4D5 is called RAID1 and comprises a cluster of residues extending from Asn22 to Leu38. Within this region the Asn22/Pro23/Trp24/Asn26 grouping and a series of hydrophobic amino acids — Val30, Leu33 and Leu37 — are essential for the interaction with RACK1 [40,41]. In contrast, a more extended section of the PDE4D5 N-terminal sequence, including several amino acids from RAID1 but extending from Thr11 to Ala85, mediates the interaction with βarrestin [40], and this appears to bind to two regions in the βarrestin C-domain [61].

Here we analyse the function and structure of a 38-mer peptide, comprising residues 12–49 of PDE4D5, which contains both the entire RACK1 interaction specificity motif, RAID1, and part of the βarrestin-interacting region [40,41].

We used the programs AGADIR [71] and PHD [72] to predict the structure of the peptide in water and within the intact protein, respectively. AGADIR predicted low (5%) α-helicity for the peptide in water, while PHD predicted a high probability of α-helix spanning residues Asn26 through to Thr45 in the protein.

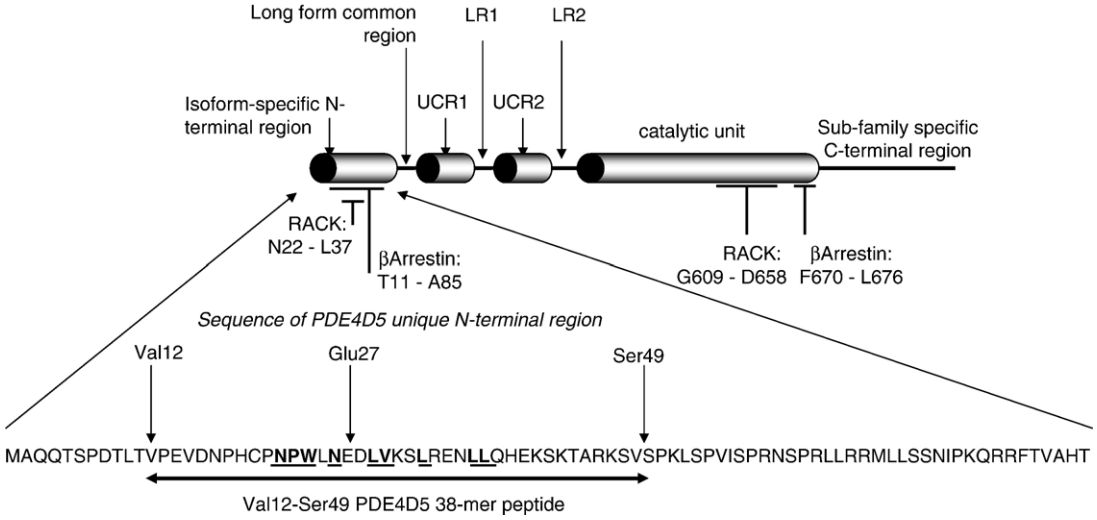

Fig. 1. The unique N-terminal region of PDE4D5. This shows schematically the domain structure of the PDE4D5 long isoform together with the amino acid sequence (GenBank™ accession number AF012073) of its unique 88 residue N-terminal region. Indicated by a horizontal arrow is the sequence of the 38-mer peptide evaluated here. In bold typeface are shown the residues of the essential Asn22/Pro23/Trp24/Asn26 grouping and also those that form the essential hydrophobic ridge, Leu29, Val30, Leu33, Leu37 and Leu38.

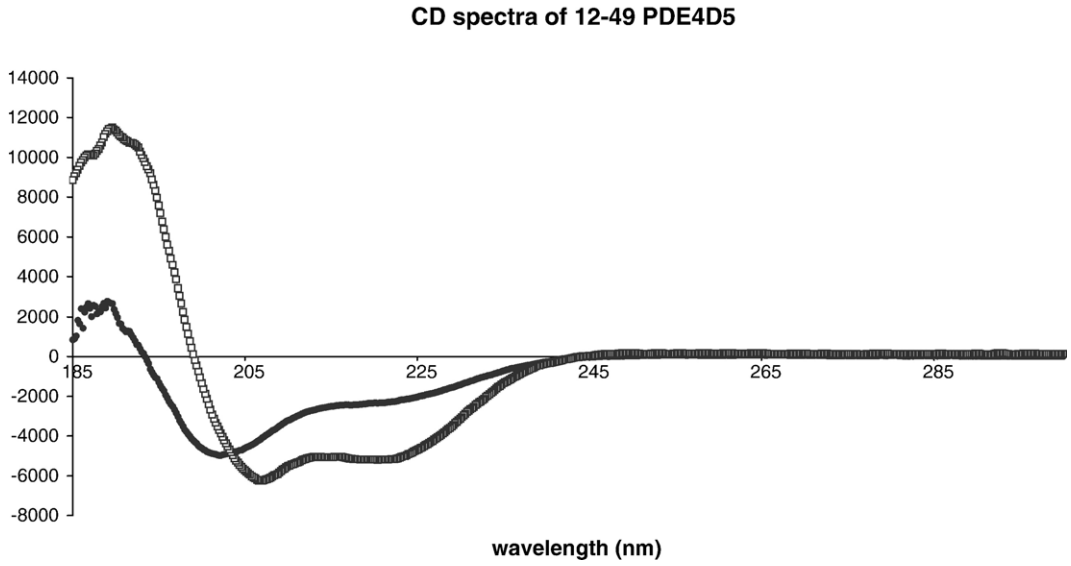

Fig. 2. CD spectra of peptide 12–49 of PDE4D5. CD spectra of peptide 12–49 at 25 °C in 10 mM phosphate buffer, pH 5.8 (circles) and in 50% phosphate buffer, pH 5.8/50% trifluoroethanol (TFE) (open squares).

3.1. Circular dichroism (CD) analysis of the RAID1-containing 38-mer PDE4D5 peptide 12–49

To gain insight into the secondary structure of the 38-mer peptide (comprising residues 12–49 of PDE4D5) at low concentrations, we analysed CD spectra (Fig. 2). Spectra taken in 10 mM phosphate buffer at 25 °C showed little regular secondary structure, resembling that of a random coil, as predicted by AGADIR. In 50% TFE the spectrum of the peptide is like that of an α-helix with minima at 222 nm and 207 nm. From the molar residue ellipticity at 222 nm the percentage α-helix under these conditions is 18%.

The impact of TFE on protein structure is controversial [73]. While TFE has a reputation for promoting α-helix, there are many reports of β-strands in TFE. TFE is thought likely not to change the intrinsic structure of the protein/peptide but, rather, to stabilise the secondary structure for which a sequence has propensity [73]. The α-helical component of the isolated RAID1 peptide might, however, arise from a small part of the peptide locked in α-helical conformation or a larger area of the peptide existing as α-helix/coil equilibrium. To examine which regions of the peptide have a propensity for α-helix formation and may therefore adopt α-helical structure in complex with either βarrestin or RACK1, we examined the structure of the peptide in 50% TFE by NMR spectroscopy.

3.2. ^{1}H NMR-determined structure of the RAID1-containing 38-mer PDE4D5 peptide 12–49

We set out to determine the structure of the 12–49 region of PDE4D5 by ^{1}H NMR spectroscopy. The resonances of the peptide were assigned to amino acid type by TOCSY and COSY [74,75]. Sequential NOEs were identified along the peptide backbone, enabling sequence specific assignments. Ambiguities due to resonance overlap were resolved by examining the spectra at different temperatures.

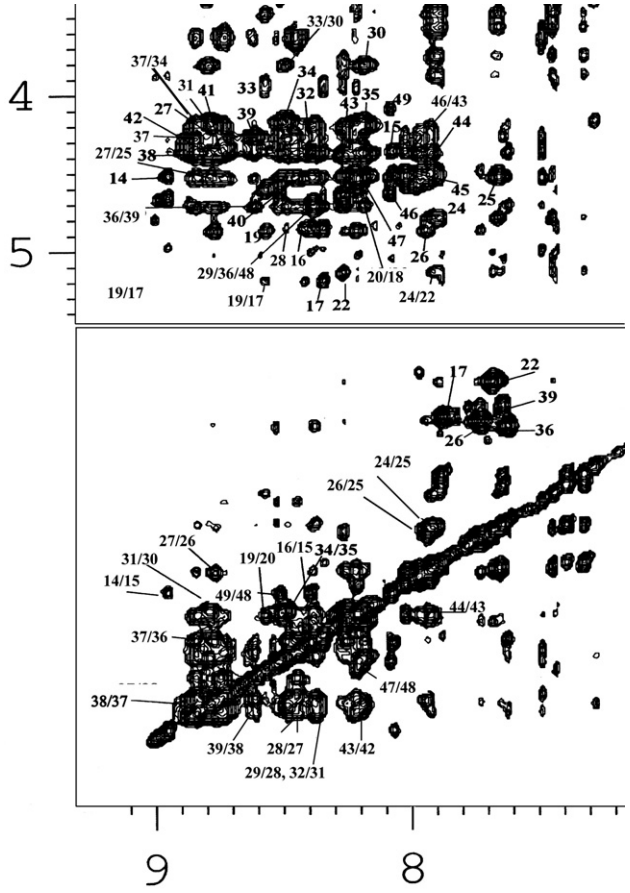

Fig. 3. Sections from NOESY spectra for peptide 12–49 of PDE4D5. Sections from the NOESY spectrum (200 ms of mixing time) for peptide 12–49 were collected in 50% TFE/50% H_2O (v/v), pH 5.8, 293 K. NOEs corresponding to connectivities within a single residue are labelled with a single number (*e.g.*, 24 refers to an NOE within residue Trp24). Inter-residue connectivities are labelled with both residue numbers. Amide to side chain connectivities, all dN(i,i+1) and some long-range dN(i,i+3) connectivities are labelled.

Fig. 4. Summary of the NOEs observed for peptide 12–49 of PDE4D5. An illustration of the sequential and medium range NOE connectivities for the peptide in 50% TFE/50% H_2O (v/v) at 293 K is presented, as used in the calculation of structures. A small number of NOEs could not be identified with certainty. The NOEs (other i,i+2), (other i,i+3), and (other i,i+4) are those not part of the other illustrated classes. In most cases these bars represent multiple NOEs observed between different protons in the respective residues. For proline the δH protons substitute for the NH protons.

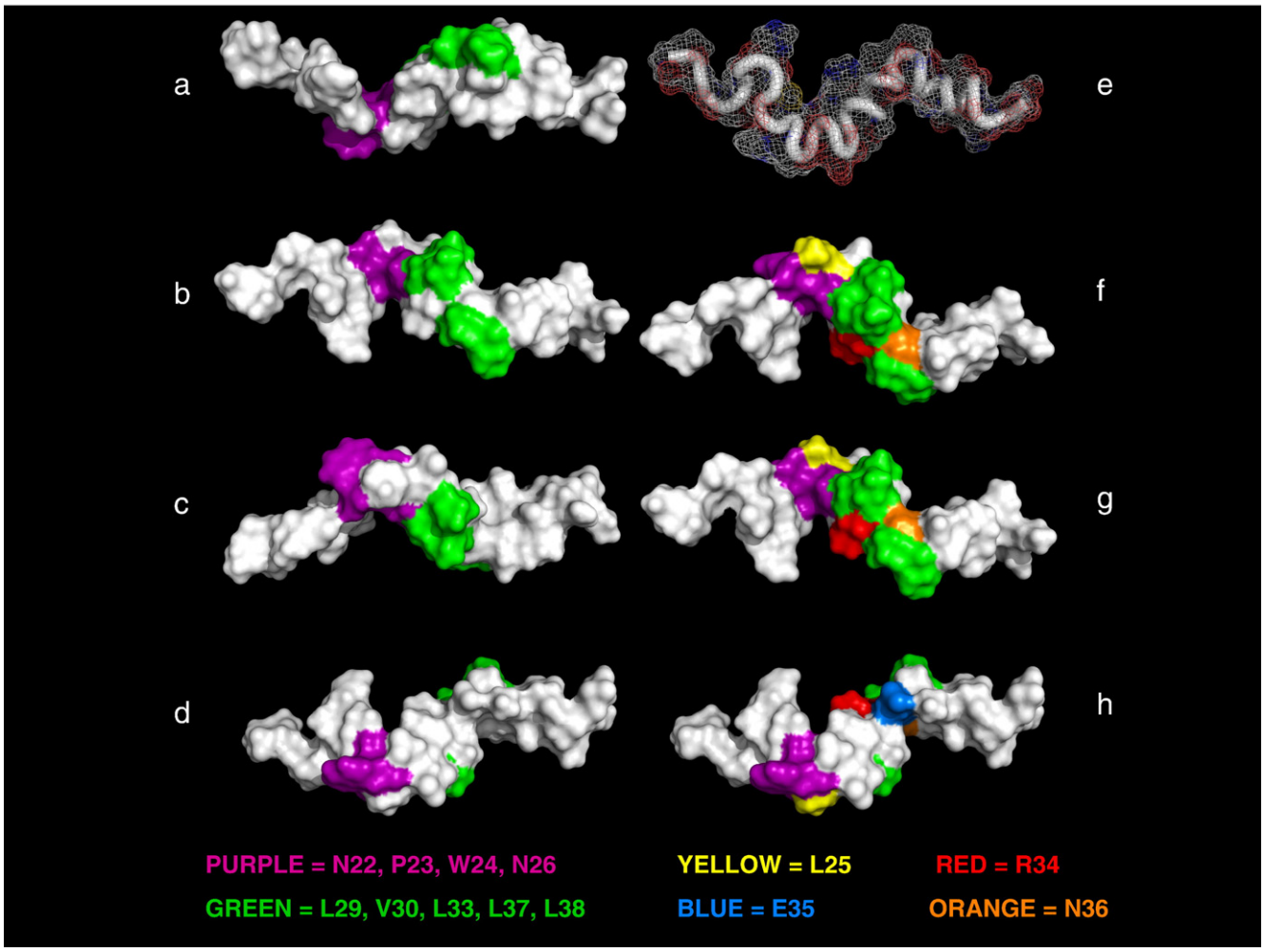

Fig. 5. Structure of the RACK1-interacting domain, RAID1, of PDE4D5. Rendered surfaces of the average ^{1}H NMR-derived structure of the 38-mer peptide, comprising residues 12–49 of PDE4D5, were generated using PyMol (www.pymol.org). Panels (a–d) show four 90° rotations of the rendered peptide with residues forming the essential Asn22/Pro23/Trp24/Asn26 grouping (purple) and those of the essential hydrophobic ridge (Leu29, Val30, Leu33, Leu37, Leu38) (green). In panel (e) the peptide backbone is shown in 'worm' format. In (f–h) the positions of Leu25 (yellow), Arg34 (red), Glu35 (blue) and Asn36 (orange) are shown relative to the essential Asn22/Pro23/Trp24/Asn26 grouping (purple) and the hydrophobic ridge (Leu29, Val30, Leu33, Leu37, Leu38) (green). The PDB ID code for the co-ordinate entry is 1e9k and the NMR restraints entry is r1e9kmr.

The pattern of cross-peaks observed in a 200-ms mixing time NOESY experiment (Figs. 3 and 4) is consistent with a number of areas of α-helical structure. The N-terminal amino acids give very few NOEs, while those from Asp16 to Asn22 are principally of the type dαiNi+2, suggesting a series of turns. From Pro23-Asn26, a large number of inter-side chain NOEs, many of the type i,i+2 or i,i+3 are seen. In the region Pro23-Leu37, several NOEs including dNiNi+1, dαiNi+3 and dαiβi+3 for many of the residues, along with multiple other i,i+2, i,i+3 and i,i+4 contacts involving both side chain and backbone protons clearly indicate an ability to adopt α-helical structure, as does the reduced exchange rate of amide protons with the solvent. In the region Leu37 to Ala46 there are fewer of the classical dαiNi+3 helical NOEs. However there are many side chain/side chain and side chain/backbone NOEs of the types i,i+3 and i,i+4, suggesting α-helical structure for much of this region.

Calculations of structures consistent with the NOEs, using distance geometry in XPLOR 3.581 followed by simulated annealing, showed residues Pro23-Leu29 and Lys42-Ala46 in α-helical conformation in the majority of structures. Between Val30 and Glu41, different turns were observed in the calculated structures and they aligned poorly, though most structures showed a 3-residue turn at Glu35-Asn36. This is consistent with a flexible peptide with α-helical propensity as noted in the CD spectrum (Fig. 2). From these structures, a model of the average structure was calculated (Fig. 5), as outlined in the Materials and methods section. The model possesses a helical backbone extending from Pro23 to Asn36 with formal α-helical structure between Pro23 and Val30. The helix pitch is then loosened by a partial break down in regular i, i+4 hydrogen bonding of carbonyl and NH groups in the backbone. A disruption occurs in the helix at Leu37, caused possibly by interaction of the side chain of Asn36 with the backbone of Ser32 and/or Arg34, and precedes another short segment of α-helix from Gln39 to Ala46. Without exception, the side chains of all the hydrophobic residues over the region from Trp24 to Leu38 are exposed on one face of the amphipathic helical structure, taking a slightly spiral track

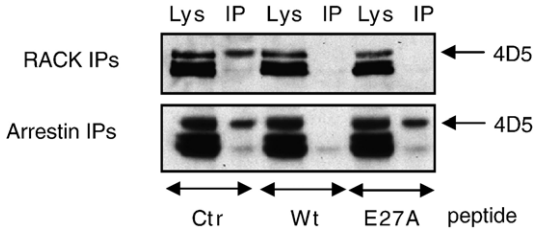

Fig. 6. Disruption of PDE4D5 interaction with RACK1 and βarrestin by a membrane-permeable, stearoylated Val12-Ser49 38-mer PDE4D5 peptide. PDE4D-specific antisera were used to probe lysates from HEKB2 cells as well as both RACK1 and βarrestin immunoprecipitates. The upper indicated band indicates the PDE4D5 isoform, confirmed by PDE4D5-specific N-terminal antisera. In the indicated instances, cells were pre-treated for 2 h with a membrane-permeable, stearoylated Val12-Ser49 38-mer peptide (WT) and a cognate peptide with a Glu27Ala substitution (E27A). This shows a typical immunoblot for an experiment done 3 times.

around the peptide (Fig. 5). This generates a pronounced hydrophobic surface formed by the side chains of Trp24, Leu25, Leu29, Val30, Leu33, Leu37 and Leu38. The polar/charged residues then flank this surface, although the side chain methylenes of Arg34 may also contribute to continuity of the hydrophobic surface between Leu33 and Leu37.

The N-terminal 4 residues are almost totally unstructured, forming a 'frayed end'. However, there are indications of structure in the N-terminal region up to residue Asn22, consisting of overlapping turns that are defined by a small number of NOEs, principally of the type dαiNi+2 (Asp16-Pro18, Asn17-His19, Pro18-Cys20, Pro21-Pro23, Asn22-Trp24). Residue Pro23, within the Asn22/Pro23/Trp24/Asn26 grouping, thus appears to initiate the well-defined amphipathic α-helical segment. Indeed, this grouping consists of an overlapping turn in which the side chains form a closely packed hydrophobic cluster that is well defined by a large number of inter-side chain NOEs, many of the type i,i+2 or i,i+3. There appear to be two backbone hydrogen bonds, formed as Pro21CO-Trp24HN and as Asn22CO-Leu25HN, in this region that contribute to the stability of the hydrophobic cluster.

In the region Pro23-Gln39, the key α-helical NOEs include strong dNiNi+1 for most residues, dαiNi+3 (Glu27-Val30, Val30-Leu33, Arg34-Leu37, Asn36-Gln39) and dαiβi+3 (Pro23-Asn26, Trp24-Glu27, Leu33-Asn36, Asn36-Gln39) along with multiple other i,i+2, i,i+3 and i,i+4 contacts involving both side chain and backbone protons. The helical backbone of this region is stabilised by hydrogen bonds of the type i,i+4 (Asn22CO-Asn26HN, Leu25CO-Leu29HN, Leu29CO-Leu33HN, Val30CO-Arg34HN, Ser32CO-Asn36HN), the presence of which are confirmed by amide protons with a reduced exchange rate with the solvent. Additional stabilisation is provided by an ion pair side chain interaction between Glu27 and Lys31. The helical region continues between residue Arg34 and Leu37 as an irregular turn that aligns poorly in different calculated structures and produces a bend in the helical region at Leu37 in the calculated average structure. This may be caused by a tendency for the side chain of Asn36 to interact with the backbone of Ser32 and/or Arg34. The region Gln39 to Ala46 then returns to regular α-helix. Although there are fewer of the classical helical NOEs (*e.g.* dαiNi+3; Ser43-Ala46) in this region, there are many side chain/side chain and side chain/backbone NOEs of the types i,i+3 and i,i+4, and these are still sufficient to define its α-helical structure. Regular α-helical hydrogen bonds are also indicated (Gln39CO-Ser43HN, His40CO-Lys44HN, Glu41CO-Thr45HN, Lys42CO-Ala46HN) and a stabilising ion pair is formed between the side chains of Glu41-Lys44. Residues Arg47-Ser49 are poorly structured, with few NOEs, forming a 'frayed' C-terminus.

3.3. Disruption of PDE4D5 interaction with RACK1 and βarrestin by a membrane-permeable, stearoylated Val12-Ser49 38-mer PDE4D5 peptide

In order to determine whether the structural integrity of RAID1 is maintained in the isolated Val12-Ser49 38-mer PDE4D5 peptide, we generated a membrane-permeable stearoylated analogue and examined its potential for disrupting complexes of PDE4D5 with βarrestin and RACK1 in HEKB2 cells. This was assessed by selectively immunoprecipitating either βarrestin or RACK1 from these cells and probing these complexes with PDE4D-specific antisera (Fig. 6). Doing this we clearly see that this peptide was able to prevent the formation/cause disruption of PDE4D5 association with both βarrestin and RACK1 (Fig. 6). Previously we have shown [40] from both scanning peptide array and mutation analyses that Glu27 is essential for PDE4D5 interaction with βarrestin. Here we show that challenge of cells with a cognate peptide, but with a Glu27Ala substitution now fails to disrupt PDE4D5 complexes with βarrestin, whilst still disrupting complexes with RACK1 (Fig. 6).

HEKB2 cells are a HEK cell line that is transfected to constitutively overexpress β_2ARs [69], which alter their cAMP signalling system [26]. One consequence of this is that isoprenaline stimulation now allows β_2ARs to activate ERK

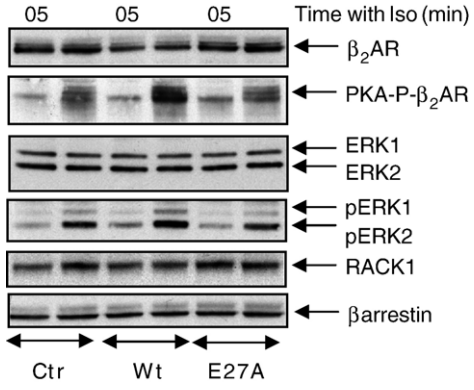

Fig. 7. Changes in PKA phosphorylation and ERK activation in isoprenaline-stimulated HEKB2 cells upon treatment with a membrane-permeable, stearoylated Val12-Ser49 38-mer PDE4D5 peptide. HEKB2 cells were challenged with isoprenaline (10 μM) for 5 min prior to harvesting and immunoblotting for the indicated species. In the indicated instances, cells were pre-treated for 2 h with a membrane-permeable, stearoylated Val12-Ser49 38-mer peptide (WT) and a cognate peptide with a Glu27Ala substitution (E27A). Shown are loading controls for the β_2AR, RACK1, ERK and βarrestin plus detection of activated, phosphorylated ERK (pERK), and PKA phosphorylated β_2AR (PKA-p-β_2AR). This shows a typical set of immunoblots for an experiment done 3 times.

entirely as a consequence of β_2ARs becoming PKA phosphorylated and thereby able to couple to G_i, as occurring in cardiomyocytes [26]. Here we confirm that β_2ARs in these cells become phosphorylated by PKA consequent to isoprenaline challenge and that this also leads to ERK activation, as indicated by an increase in pERK (Fig. 7). PKA phosphorylation of the β_2AR is determined by a PKA sub-population tethered to it by AKAP79 [45,76] and this complex is subject to negative regulation by PDE4D5 recruited to the β_2AR in complex with βarrestin [40,45]. Here we show that challenge of HEKB2 cells with the Val12-Ser49 38-mer PDE4D5 peptide, which prevents sequestration of PDE4D5 by βarrestin, led to a marked increase in the isoprenaline-induced PKA phosphorylation of the β_2AR and activation of ERK (Fig. 7). In marked contrast to this, the cognate peptide having a Glu27Ala substitution, which is unable to prevent the accumulation of βarrestin-sequestered PDE4D5, was ineffective in achieving this (Fig. 7).

Thus the Val12-Ser49 38-mer PDE4D5 peptide has functional properties, shown here in its ability to prevent desensitization of β_2AR signalling to ERK in HEKB2 cells by facilitating the isoprenaline-mediated PKA phosphorylation of the β_2ARs.

4. Discussion

The unique, isoform-specific 88 amino acid N-terminal region of PDE4D5 confers specificity in binding of this PDE4 isoform to the signal scaffold proteins, βarrestin and RACK1, which occurs in a mutually exclusive manner [40]. Whilst βarrestin binds over an extended surface of this region, from Thr11 to Ala85, RACK1 binding is focused within a compact region extending from Asn22 to Leu38, which we have called RAID1 [41]. RAID1 is formed by the Asn22/Pro23/Trp24/Asn26 grouping together with a series of essential hydrophobic residues (Val30, Leu33, Leu37) as determined by independent biochemical analyses of mutation in 2-hybrid and pull-down studies together with scanning peptide array analyses [40,41,44]. The binding of βarrestin also requires residues located within the RAID1 region, notably the Asn22/Pro23/Trp24/Asn26 grouping involved in RACK1 binding as well as Glu27, Leu33 and Arg34 [40]. Indeed, Glu27 is uniquely important for the binding of βarrestin to PDE4D5 but does not affect the binding of RACK1 to PDE4D5 [40]. In contrast to this Leu37 is uniquely important for the binding of RACK1 to PDE4D5 but does not affect the binding of βarrestin to PDE4D5 [40].

Here we have examined the structure and functional properties of a 38-mer peptide, comprising residues 12–49 of PDE4D5, which contains the entire RACK1 interaction specificity motif, RAID1. Secondary structure predictions of the peptide by AGADIR suggest that it forms little helix in aqueous solution, as seen in the CD studies in phosphate buffer (Fig. 2). However, predictions of the structure of the peptide in a protein environment by PHD, strongly suggest that the region bounded by residues Asn26-Thr45 will be α-helical.

Indeed, in the presence of 50% TFE, which may stabilise the peptide's intrinsic structure, CD studies indicated that the RAID1 sequence has significant α-helical character (Fig. 2). Further examination by ^{1}H NMR spectroscopy subsequently confirmed that the RAID1-containing peptide has a very strong propensity towards adoption of an α-helical structure. Thus, an averaged structural model, built on observed NOEs, showed a helical backbone extending from Pro23 to Ala46, with a short sequence of formal α-helix between Pro23 and Val30 followed by a rather looser helical structure to Asn36; a bend at Leu37 is then followed by a return to regular α-helix between Gln39 and Ala46. The looser helical structure found between Lys31 and Leu38 reflects conformational flexibility in the isolated peptide, with the i,i+4 α-helix hydrogen bonding of the backbone breaking and reforming in mobile equilibrium with some conformations in which side chain–backbone interactions (*e.g.* Ser32 OH…Asp28 carbonyl) partially disrupt its regular α-helical structure. Binding of the peptide to βarrestin or RACK1 is expected to restrict its conformational mobility and may stabilise regular α-helical structure over the RAID1 sequence. We believe, therefore, that this is the most likely structure adopted by this critical region of PDE4D5 when it interacts with either βarrestin or RACK1.

The extended helical structure between Pro23 and Ala46 deduced from the NMR studies correlates well with the region (Asn26-Thr45) predicted to adopt α-helical structure by PHD and encompasses all of RAID1 [40]. The critical Asn22/Pro23/Trp24/Asn26 grouping occupies the head of the helix (Fig. 5; panels a–d, f–g; purple highlight) and the essential hydrophobic L/V-region (Val30, Leu33, Leu37), together with Leu29 and Leu38, forms an extremely well-defined hydrophobic ridge (Fig. 5; panels a–d, f–g; green highlight) that tracks a slightly spiral course over one face of the helical peptide. This hydrophobic ridge (Fig. 5; panels a–d, f–g; green highlight) appears to comprise three key sticky 'patches'; 'patch 1' being formed by Leu29 and Val30, 'patch 2' by Leu33 and 'patch 3' by Leu37 and Leu38. Destruction of any one of these patches in its entirety suffices to ablate interaction with RACK1 [40]. However, single mutations, to the charged amino acid aspartate, within either patch 1 or patch 3 are not sufficient to ablate interaction of PDE4D5 with RACK1. Leu25 (Fig. 5; panel f; yellow) appears to form a simple continuation of this hydrophobic ridge into the essential Asn22/Pro23/Trp24/Asn26 grouping. However, its mutagenesis to a range of charged and aromatic amino acids did not affect the ability of PDE4D5 to interact with RACK1 [40,41], suggesting that it has little or no role in determining the interaction between these two proteins. Thus the Asn22/Pro23/Trp24/Asn26 grouping and the hydrophobic ridge that encompasses Leu29, Val30, Leu33, Leu37 and Leu38 appear to form two discrete units within RAID1 that are each essential for PDE4D5 to bind to RACK1.

Previously we also found that mutation of either Arg34 or Asn36 to alanine severely attenuated interaction of PDE4D5 with RACK1 [40,41]. Interestingly these two residues (Fig. 5, panels f–h; respectively red and orange highlight) are orientated on either side of and immediately flank the hydrophobic ridge on the RAID1 helix. Given this presentation, it is feasible that Arg34 and Asn36 also make direct contact upon docking of the RAID1 hydrophobic ridge to its binding site on RACK1. These

residues may therefore contribute hydrogen bonds and/or a salt bridge or pi–cation interactions (in the case of Arg34) to the target surface on RACK1. However, the side chain methylenes of Arg34 are also part of a contiguous surface bridging between patches 2 and 3 of the RAID1 hydrophobic ridge. Thus it is also possible that the Arg34 side chain provides an important hydrophobic contribution to the association of the PDE4D5 RAID1 sequence with RACK1. As the Arg34 and Asn36 residues appear to precede a bend in the structure of the isolated 38-mer peptide examined here, we cannot strictly eliminate the possibility that their importance for RACK1 binding arises indirectly as a consequence of the role they may play in controlling the overall conformation of the peptide. However, it is significant that Glu35 (Fig. 5, panels f–h; blue highlight), which is adjacent to Arg34 and Asn36, but orientated on the opposite side of the helix to the hydrophobic ridge, appears to have no involvement in PDE4D5/RACK1 interaction according to our earlier mutation studies and peptide array analysis [40,41].

The WD-repeat protein G_β interacts with the G_γ protein through coiled-coil interactions [77,78]. The key to this is the generation of a hydrophobic surface along one face of each of the helices contributed by both partners. It is thus very interesting to find here that a hydrophobic ridge located on a single face of an α-helical region is essential for the binding of PDE4D5 to RACK1, which also belongs to the WD-repeat family. Significantly, helix–helix interactions have been shown [79–81] to be particularly favoured if repeating functional leucine residues have a C-terminal adjacent residue that alternates with uncharged and charged residues as in a 'Leu/apolar-$(X_{aa})_n$-Leu/polar-$(X_{aa})_n$-Leu/apolar' amino acid repeat. Just such a scenario is presented in PDE4D5, with mutagenesis studies identifying the sequence Leu29, Val30, X_{aa}, X_{aa}, Leu33, Arg34, X_{aa}, X_{aa}, Leu37, Leu38. This is consistent with the potential importance of Arg34 in RACK1/PDE4D5 interaction.

It has been suggested that helical units involved in protein–protein interactions may perform a crucial role in orientating functional groups located at the head of the helices [82]. Thus, in RAID1, the essential hydrophobic ridge may provide the driving force for an initial helix–helix interaction that is then further stabilised through the correct presentation of the essential Asn22/Pro23/Trp24/Asn26 grouping found at the N-terminal head of this helical region. It should be noted, however, that residues within this grouping may also have a particular role in serving to initiate the formation of the particular helix upon which the hydrophobic ridge is located.

RAID1 is thus made up of a number of elements, which are all essential for the effective binding of PDE4D5 to RACK1. These are (i) the Asn22/Pro23/Trp24/Asn26 grouping found at the head of an amphipathic helix; (ii) a hydrophobic ridge formed from 3 key sticky patches, involving Leu29 and Val30 in the first, Leu33 in the second and Leu37 and Leu38 in the third; and (iii) an essential/enhancing contribution from Arg34 and Asn36 which flank either side of the hydrophobic ridge. Structural features of the PDE4D5 RAID1 sequence suggest that its binding to RACK1 could involve helix–helix interactions akin to those seen for the binding of the G_γ protein to G_β. To date, however, the crystal structure of RACK1 has not been determined, and it has not been established whether the protein has an N-terminal α-helix analogous to that seen in G_β. Sequence alignment and homology modeling [43] suggest that RACK1 may in fact lack such a helix, which would then require RAID1 to adopt a distinct mode of interaction and either align along the protein's beta-propeller blades or fold across one of its two propeller faces.

In contrast to the compact RAID1 motif, a more extensive sequence, spanning nearly the entirety of the unique, 88 residue isoform-specific N-terminal region of PDE4D5, has been implicated in this enzyme's association with βarrestin [40,41]. This sequence stretches from Thr11 to Ala85 and, therefore, encompasses and extends beyond the 38-mer peptide that we analyse here. Nevertheless, we have previously shown through mutational analysis and peptide array studies that several residues within the 38-mer peptide play key roles in the binding of PDE4D5 to βarrestin. Thus, Glu27Ala, Leu33Ala or Arg34Ala mutations individually serve to ablate βarrestin binding in the intact PDE4D5 enzyme, whilst the individual replacement of a number of other residues — Asn26, Asp28, Leu29, Val30 — severely compromises the association of the two proteins [40]. These amino acids clearly include several of those implicated in the binding of PDE4D5 to RACK1, and it is for this reason that the associations of the enzyme with RACK1 and βarrestin are mutually exclusive [40]. Indeed, the particular residue set implicated in βarrestin binding suggests that this scaffolding protein binds to the same face of the RAID1 helix to which RACK1 docks. In contrast to the interaction with RACK1, however, the residues required for βarrestin binding form a more tightly focused band around the helix (Fig. 8). The core of the βarrestin-interacting surface again features an extensive hydrophobic area, albeit less pronounced than the extended ridge presented by the RAID1 surface for interaction with RACK1. In this case the relevant hydrophobic zone is formed by Leu29, Val30, Leu33 (Fig. 8, panels e–h; green highlight) and possibly by the side chain methylenes of Arg34 (Fig. 8, panels e–h; red highlight); the extended surface provided by Leu37/Leu38 for interaction with RACK1 is not required for βarrestin binding. The hydrophobic core surface is then flanked by polar/charged residues (Asn26, Glu27, Asp28, and the terminal guanidinium functionality of Arg34). Of these latter residues, Glu27 and Asp28 are uniquely required for βarrestin binding but not for association with RACK1.

The structure of the overall βarrestin-interacting surface is such that it may bind to a deep groove or cleft in the βarrestin surface, conceivably with a complementary hydrophobic surface in its floor. Alternatively, the side chains of Leu29, Val30 and Leu33 may be presented to a hydrophobic pit in the βarrestin surface, with the flanking polar/charged residues (Asn26, Asp28 and Arg34) forming interactions to complementary amino acids around the rim of the pit. Direct contact with six of the seven residues (Asn26, Asp28, Leu29, Val30, Leu33 Arg34) involved in the interaction with βarrestin should be possible by open contact between the surfaces of βarrestin and PDE4D5. Intriguingly the seventh residue (Glu27) is located on the opposite side of the helix to the hydrophobic patch. Simultaneous direct surface contact with Glu27, which is

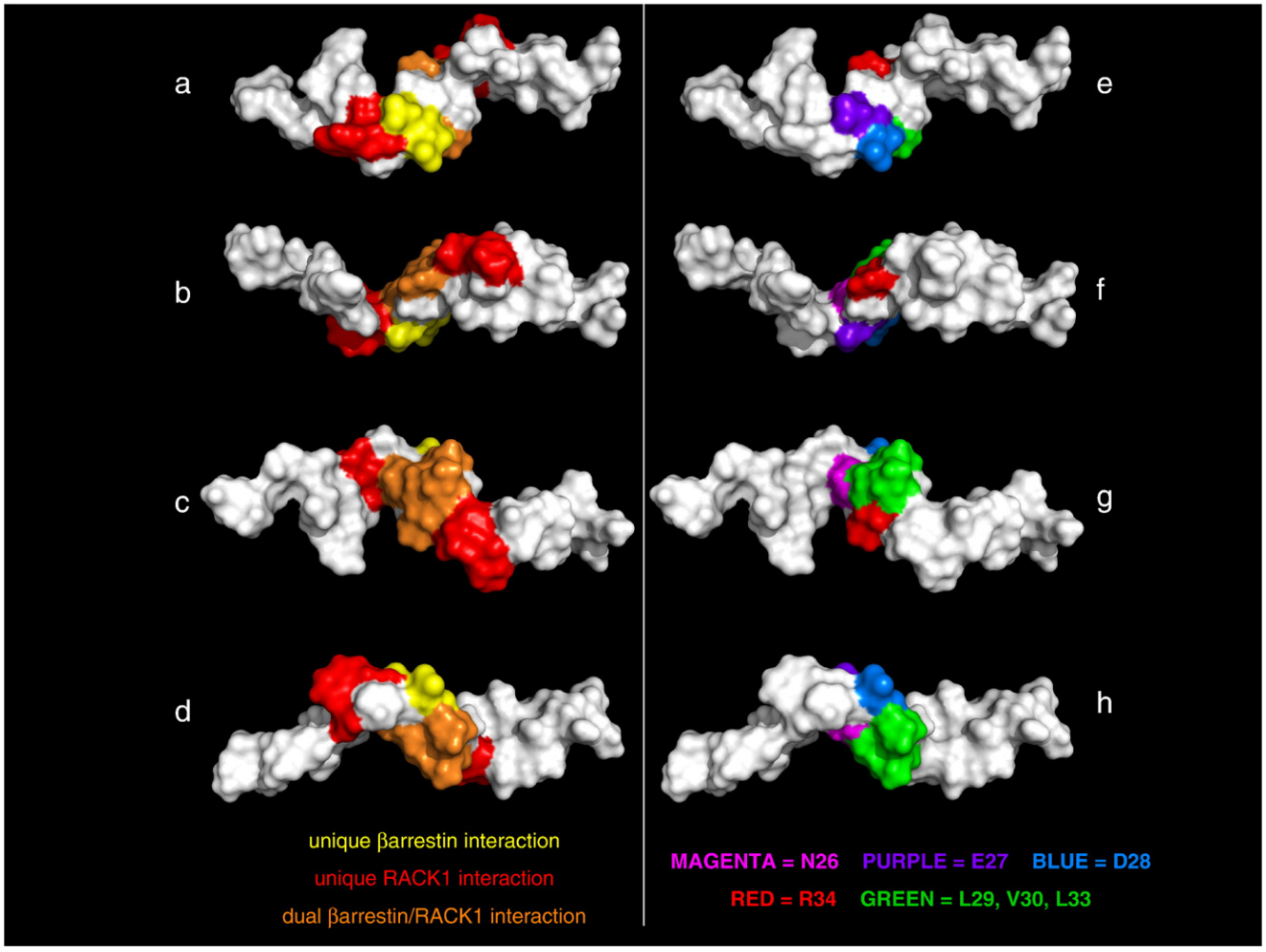

Fig. 8. Location and relation of βarrestin-interacting residues relative to RACK1-interacting residues in the PDE4D5 RAID1 sequence. Rendered surfaces of the average ^{1}H NMR-derived structure of the 38-mer peptide, comprising residues 12–49 of PDE4D5, were generated using PyMol (www.pymol.org). Panels (a–d) show four 90° rotations with the residues uniquely required for RACK1 interaction shown in red, residues uniquely required for βarrestin interaction shown in yellow and residues contributing to interaction with both proteins shown in orange. Panels (e–h) show the same set of views as panels (a–d) but highlight the residues implicated in βarrestin binding: Asn26 (magenta); Glu27 (purple); Asp28 (blue); Arg34 (red); Leu29, Val30 and Leu33 (green).

a residue essential for βarrestin binding, would require βarrestin to wrap around some 270° of the helical PDE4D5 peptide at this point. Thus, if the helical structure of the PDE4D5 peptide is preserved at this location when bound to βarrestin, this would suggest that βarrestin undergoes a conformational change upon PDE4D5 binding so as to partially encase the bound peptide sequence.

We have previously identified [61] two regions in the C-domain of βarrestin2 that are essential for interaction with the PDE4D5 N-terminus. These are a section of β-sheet (Leu215-His220) on the exposed convex face of the βarrestin C-domain together with residues Arg286 and Asp291, which are located close to the key phosphate sensor (Arg170) in the polar core of βarrestin [55,83,84]. Neither of these locations in the basal conformation of βarrestin, the structure of which has been determined by X-ray crystallography [85–88], appears to provide a complementary surface to which the helical peptide motif encompassing Asn26-Val30, Leu33 and Arg34 might bind. We note, however, that βarrestin can undergo profound conformational change upon binding to partner proteins. Thus, recruitment of βarrestin to phospho-GPCR is associated with a hinged re-orientation of the βarrestin N- and C-domains in a conformational change that requires displacement of the protein's C-terminal sequence from the position it adopts in the basal state, folded over β-strands 1 and 2 of the N-domain [55,83,84]. A similar displacement of the βarrestin C-terminal 'latch' sequence was invoked in our earlier studies to map βarrestin residues involved in binding of PDE4D5 [61]. Given this potential for conformational reorganization, it is possible that the βarrestin binding site for the PDE4D5 helical peptide containing Asn26-Val30, Leu33 and Arg34 is immature in the basal state to which the available βarrestin crystal structures correspond. Induced movement in the βarrestin structure upon PDE4D5 binding may thus be required to establish a complementary binding surface for this section of the PDE4D5 N-terminus. Thus, as suggested previously by us, PDE4D5 binding may either elicit or require a conformational change in βarrestin [40,61].

We have suggested that one means of addressing the issue of trying to inhibit specific PDE4 isoforms is to displace them from

functionally relevant sites in cells (see *e.g.* [5,8,9,13,26]). Proof of principle for this has been demonstrated by our dominant negative strategy where overexpression of a catalytically inactive form of PDE4D5 has been used to displace specific active endogenous sub-populations of PDE4D5 from the scaffolding proteins RACK1 and βarrestin in various cell types [40,45,58]. Mutations made in catalytically inactive PDE4D5 can then be used to target displacement specifically to one or other of these scaffolds. In displacing endogenous, active PDE4D5 we were able to generate an overt phenotype, namely an increase in the isoprenaline-stimulated phosphorylation of the β_2AR achieved by a PKA sub-population that is sequestered to the β_2AR through AKAP79. Here we show that we can recapitulate this action using a cell-permeable peptide, namely the Val12-Ser49 38-mer PDE4D5 from the unique N-terminal region of PDE4D5 (Fig. 7). Whilst this peptide can displace both RACK1 and βarrestin-sequestered PDE4D5, its ability to accentuate the isoprenaline-stimulated PKA phosphorylation of the β_2AR was ablated upon Glu27Ala substitution, which selectively negates its interaction with βarrestin. These data not only indicate that cell-permeable peptides, and perhaps peptidomimetics and small molecules, can be used to disrupt the interaction of PDE4 species with scaffold proteins, but are also consistent with our demonstration here that the isolated Val12-Ser49 38-mer PDE4D5 can adopt a functionally relevant structure. The physical analyses performed here are consistent with predictions that this peptide has the propensity to form a functionally active structure, which we suggest here has a flexible helical nature. Such a helical structure appears to allow it to present, on a defined surface, those amino acids identified in various independent approaches as being involved in its binding to either RACK1 or βarrestin [40]. Recently, we have used cell-permeable peptides identified from peptide array analyses to disrupt interactions between PDE4A4 and the p75 neurotropin receptor involved in regulating fibrin deposition and scarring in lung disease [89], as well as between PDE4D3 and the scaffold protein DISC1, involved in schizophrenia [90]. These data indicate the potential for exploiting disruption of the interaction between PDE4 isoforms and their anchor proteins to give functional insight into the role of specifically tethered sub-populations of various PDE4 isoforms as well as for potential therapeutic exploitation.

Acknowledgements

This work was supported by the Medical Research Council (U.K.) grants G8604010 and G0400053 (MDH); European Union Grant 037189 (EK and MDH); Fondation Leducq 06 CVD 02 (MDH); Deutsche Forschungsgemeinschaft grant Kl1415/2 and 4/1 (EK); by the NIH R01-GM58553 (GBB) and by Capital Equipment Grants 068232/Z/02/Z and 056432 from the Wellcome Trust for the NMR facilities.

References

[1] F.D. Smith, L.K. Langeberg, J.D. Scott, Trends Biochem. Sci. 31 (6) (2006) 316.
[2] K. Taskén, E.M. Aandahl, Physiol. Rev. 84 (1) (2004) 137.
[3] S.S. Taylor, J. Yang, J. Wu, N.M. Haste, E. Radzio-Andzelm, G. Anand, Biochim. Biophys. Acta. 1697 (1–2) (2004) 259.
[4] W. Wong, J.D. Scott, Nat. Rev., Mol. Cell Biol. 5 (12) (2004) 959.
[5] M.D. Houslay, G. Milligan, Trends Biochem. Sci. 22 (6) (1997) 217.
[6] M. Conti, J. Beavo, Annu. Rev. Biochem. 76 (2007) 481.
[7] M. Conti, W. Richter, C. Mehats, G. Livera, J.Y. Park, C. Jin, J. Biol. Chem. 278 (8) (2003) 5493.
[8] M.D. Houslay, D.R. Adams, Biochem. J. 370 (Pt 1) (2003) 1.
[9] M.D. Houslay, G.S. Baillie, D.H. Maurice, Circ. Res. 100 (7) (2007) 950.
[10] V. Boswell-Smith, D. Spina, C.P. Page, Br. J. Pharmacol. 147 (2006) S252.
[11] Z. Huang, J.A. Mancini, Curr. Med. Chem. 13 (27) (2006) 3253.
[12] J.M. O'Donnell, H.T. Zhang, Trends Pharmacol. Sci. 25 (3) (2004) 158.
[13] M.D. Houslay, Prog. Nucleic Acid Res. Mol. Biol. 69 (2001) 249.
[14] M.D. Houslay, M. Sullivan, G.B. Bolger, Adv. Pharmacol. 44 (1998) 225.
[15] I.R. Le Jeune, M. Shepherd, G. Van Heeke, M.D. Houslay, I.P. Hall, J. Biol. Chem. 277 (39) (2002) 35980.
[16] L. Monaco, E. Vicini, M. Conti, J. Biol. Chem. 269 (1) (1994) 347.
[17] E. Vicini, M. Conti, Mol. Endocrinol. 11 (7) (1997) 839.
[18] D.A. Wallace, L.A. Johnston, E. Huston, D. MacMaster, T.M. Houslay, Y.F. Cheung, L. Campbell, J.E. Millen, R.A. Smith, I. Gall, R.G. Knowles, M. Sullivan, M.D. Houslay, Mol. Pharmacol. 67 (6) (2005) 1920.
[19] G. Rena, F. Begg, A. Ross, C. MacKenzie, I. McPhee, L. Campbell, E. Huston, M. Sullivan, M.D. Houslay, Mol. Pharmacol. 59 (5) (2001) 996.
[20] Y. Shakur, J.G. Pryde, M.D. Houslay, Biochem. J. 292 (Pt 3) (1993) 677.
[21] Y. Shakur, M. Wilson, L. Pooley, M. Lobban, S.L. Griffiths, A.M. Campbell, J. Beattie, C. Daly, M.D. Houslay, Biochem. J. 306 (Pt 3) (1995) 801.
[22] E. Huston, I. Gall, T.M. Houslay, M.D. Houslay, J. Cell. Sci. 119 (Pt 18) (2006) 3799.
[23] G. Scotland, M.D. Houslay, Biochem. J. 308 (Pt 2) (1995) 673.
[24] K.J. Smith, G. Scotland, J. Beattie, I.P. Trayer, M.D. Houslay, J. Biol. Chem. 271 (28) (1996) 16703.
[25] E. Huston, T.M. Houslay, G.S. Baillie, M.D. Houslay, Biochem. Soc. Trans. 34 (Pt 4) (2006) 504.
[26] G.S. Baillie, M.D. Houslay, Curr. Opin. Cell. Biol. 17 (2) (2005) 129.
[27] G.S. Baillie, J.D. Scott, M.D. Houslay, FEBS Lett. 579 (15) (2005) 3264.
[28] H. Abrahamsen, G. Baillie, J. Ngai, T. Vang, K. Nika, A. Ruppelt, T. Mustelin, M. Zaccolo, M. Houslay, K. Taskén, J. Immunol. 173 (8) (2004) 4847.
[29] M. Mongillo, T. McSorley, S. Evellin, A. Sood, V. Lissandron, A. Terrin, E. Huston, A. Hannawacker, M.J. Lohse, T. Pozzan, M.D. Houslay, M. Zaccolo, Circ. Res. 95 (1) (2004) 67.
[30] M. Mongillo, C.G. Tocchetti, A. Terrin, V. Lissandron, Y.F. Cheung, W.R. Dostmann, T. Pozzan, D.A. Kass, N. Paolocci, M.D. Houslay, M. Zaccolo, Circ. Res. 98 (2) (2006) 226.
[31] A. Terrin, G. Di Benedetto, V. Pertegato, Y.F. Cheung, G. Baillie, M.J. Lynch, N. Elvassore, A. Prinz, F.W. Herberg, M.D. Houslay, M. Zaccolo, J. Cell Biol. 175 (3) (2006) 441.
[32] D. Willoughby, W. Wong, J. Schaack, J.D. Scott, D.M. Cooper, EMBO. J. 25 (10) (2006) 2051.
[33] F. Rochais, A. Abi-Gerges, K. Horner, F. Lefebvre, D.M. Cooper, M. Conti, R. Fischmeister, G. Vandecasteele, Circ. Res. 98 (8) (2006) 1081.
[34] T.C. Rich, W. Xin, C. Mehats, K.A. Hassell, L.A. Piggott, X. Le, J.W. Karpen, M. Conti, Am. J. Physiol., Cell Physiol. 292 (1) (2007) C319.
[35] G. Bolger, T. Michaeli, T. Martins, T. St John, B. Steiner, L. Rodgers, M. Riggs, M. Wigler, K. Ferguson, Mol. Cell Biol. 13 (10) (1993) 6558.
[36] M.B. Beard, A.E. Olsen, R.E. Jones, S. Erdogan, M.D. Houslay, G.B. Bolger, J. Biol. Chem 275 (14) (2000) 10349.
[37] S.J. MacKenzie, G.S. Baillie, I. McPhee, G.B. Bolger, M.D. Houslay, J. Biol. Chem 275 (22) (2000) 16609.
[38] C. Sette, M. Conti, J. Biol. Chem. 271 (28) (1996) 16526.
[39] G.B. Bolger, S. Erdogan, R.E. Jones, K. Loughney, G. Scotland, R. Hoffmann, I. Wilkinson, C. Farrell, M.D. Houslay, Biochem. J. 328 (Pt 2) (1997) 539.
[40] G.B. Bolger, G.S. Baillie, X. Li, M.J. Lynch, P. Herzyk, A. Mohamed, L.H. Mitchell, A. McCahill, C. Hundsrucker, E. Klussmann, D.R. Adams, M.D. Houslay, Biochem J 398 (1) (2006) 23.
[41] G.B. Bolger, A. McCahill, S.J. Yarwood, M.S. Steele, J. Warwicker, M.D. Houslay, BMC Biochem. 3 (1) (2002) 24.

[42] A. McCahill, J. Warwicker, G.B. Bolger, M.D. Houslay, S.J. Yarwood, Mol. Pharmacol. 62 (6) (2002) 1261.
[43] M.R. Steele, A. McCahill, D.S. Thompson, C. MacKenzie, N.W. Isaacs, M.D. Houslay, G.B. Bolger, Cell. Signal. 13 (7) (2001) 507.
[44] S.J. Yarwood, M.R. Steele, G. Scotland, M.D. Houslay, G.B. Bolger, J. Biol. Chem. 274 (21) (1999) 14909.
[45] M.J. Lynch, G.S. Baillie, A. Mohamed, X. Li, C. Maisonneuve, E. Klussmann, G. van Heeke, M.D. Houslay, J. Biol. Chem. 280 (39) (2005) 33178.
[46] D. Ron, C.H. Chen, J. Caldwell, L. Jamieson, E. Orr, D. Mochly-Rosen, Proc. Natl. Acad. Sci. U. S. A. 91 (3) (1994) 839.
[47] E.A. Cox, D. Bennin, A.T. Doan, T. O'Toole, A. Huttenlocher, Mol. Biol. Cell 14 (2) (2003) 658.
[48] A.M. Gaboreanu, R. Hrstka, W. Xu, M. Shy, J. Kamholz, J. Lilien, J. Balsamo, J. Cell Biol. 177 (4) (2007) 707.
[49] L. Hu, F. Lu, Y. Wang, Y. Liu, D. Liu, Z. Jiang, C. Wan, B. Zhu, L. Gan, Y. Wang, Z. Wang, J. Mol. Neurosci. 29 (1) (2006) 55.
[50] C.K. Isacson, Q. Lu, R.H. Karas, D.H. Cox, Am. J. Physiol., Cell Physiol. 292 (4) (2007) C1459.
[51] Y.V. Liu, J.H. Baek, H. Zhang, R. Diez, R.N. Cole, G.L. Semenza, Mol. Cell 25 (2) (2007) 207.
[52] I. Onishi, P.J. Lin, G.H. Diering, W.P. Williams, M. Numata, Cell. Signal. 19 (1) (2007) 194.
[53] A. Zakrzewicz, M. Hecker, L.M. Marsh, G. Kwapiszewska, B. Nejman, L. Long, W. Seeger, R.T. Schermuly, N.W. Morrell, R.E. Morty, O. Eickelberg, Circulation 115 (23) (2007) 2957.
[54] W. Zhang, C.S. Zong, U. Hermanto, P. Lopez-Bergami, Z. Ronai, L.H. Wang, Mol. Cell Biol. 26 (2) (2006) 413.
[55] E.V. Gurevich, V.V. Gurevich, Genome Biol. 7 (9) (2006) 236.
[56] S.M. DeWire, S. Ahn, R.J. Lefkowitz, S.K. Shenoy, Annu. Rev. Physiol. 69 (2007) 483.
[57] P.H. McDonald, R.J. Lefkowitz, Cell Signal 13 (10) (2001) 683.
[58] G.S. Baillie, A. Sood, I. McPhee, I. Gall, S.J. Perry, R.J. Lefkowitz, M.D. Houslay, Proc. Natl. Acad. Sci. U. S. A. 100 (3) (2003) 940.
[59] G.B. Bolger, A. McCahill, E. Huston, Y.F. Cheung, T. McSorley, G.S. Baillie, M.D. Houslay, J. Biol. Chem. 278 (49) (2003) 49230.
[60] S.J. Perry, G.S. Baillie, T.A. Kohout, I. McPhee, M.M. Magiera, K.L. Ang, W.E. Miller, A.J. McLean, M. Conti, M.D. Houslay, R.J. Lefkowitz, Science 298 (5594) (2002) 834.
[61] G.S. Baillie, D.R. Adams, N. Bhari, T.M. Houslay, S. Vadrevu, D. Meng, X. Li, A. Dunlop, G. Milligan, G.B. Bolger, E. Klussmann, M.D. Houslay, Biochem. J. 404 (1) (2007) 71.
[62] R.J. Lefkowitz, K.L. Pierce, L.M. Luttrell, Mol. Pharmacol. 62 (5) (2002) 971.
[63] M.D. Houslay, P. Schafer, K.Y. Zhang, Drug Discov. Today 10 (22) (2005) 1503.
[64] A.T. Brünger, G.M. Clore, A.M. Gronenborn, R. Saffrich, M. Nilges, Science 261 (5119) (1993) 328.
[65] S.A. White, M. Nilges, A. Huang, A.T. Brünger, P.B. Moore, Biochemistry 31 (6) (1992) 1610.
[66] L. Zhong, W.C. Johnson Jr, Proc. Natl. Acad. Sci. U. S. A. 89 (10) (1992) 4462.
[67] R. Frank, J. Immunol. Methods 267 (1) (2002) 13.
[68] A. Kramer, J. Schneider-Mergener, Methods Mol. Biol. 87 (1998) 25.
[69] A.J. McLean, G. Milligan, Br. J. Pharmacol. 130 (8) (2000) 1825.
[70] M.M. Bradford, Anal. Biochem. 72 (1976) 248.
[71] V. Muñoz, L. Serrano, Biopolymers 41 (5) (1997) 495.
[72] B. Rost, Methods Enzymol. 266 (1996) 525.
[73] M. Buck, Q. Rev. Biophys. 31 (3) (1998) 297.
[74] L. Ernst, Nucleic Acids Res. 15 (1) (1987) 361.
[75] D. Marion, K. Wüthrich, Biochem. Biophys. Res. Commun. 113 (3) (1983) 967.
[76] I.D.C. Fraser, M. Cong, J. Kim, E.N. Rollins, Y. Daaka, R.J. Lefkowitz, J.D. Scott, Curr. Biol. 10 (7) (2000) 409.
[77] J. Sondek, A. Bohm, D.G. Lambright, H.E. Hamm, P.B. Sigler, Nature 379 (6563) (1996) 369.
[78] M.A. Wall, D.E. Coleman, E. Lee, J.A. Iñiguez-Lluhi, B.A. Posner, A.G. Gilman, S.R. Sprang, Cell 83 (6) (1995) 1047.
[79] N.E. Zhou, C.M. Kay, R.S. Hodges, Protein Eng. 7 (11) (1994) 1365.
[80] D. Krylov, I. Mikhailenko, C. Vinson, EMBO J. 13 (12) (1994) 2849.
[81] W.D. Kohn, C.M. Kay, R.S. Hodges, J. Mol. Biol. 267 (4) (1997) 1039.
[82] O.D. Monera, N.E. Zhou, P. Lavigne, C.M. Kay, R.S. Hodges, J. Biol. Chem. 271 (8) (1996) 3995.
[83] V.V. Gurevich, E.V. Gurevich, Trends Pharmacol. Sci. 25 (2) (2004) 105.
[84] V.V. Gurevich, E.V. Gurevich, Pharmacol. Ther. 110 (3) (2006) 465.
[85] J. Granzin, U. Wilden, H.W. Choe, J. Labahn, B. Krafft, G. Büldt, Nature 391 (6670) (1998) 918.
[86] M. Han, V.V. Gurevich, S.A. Vishnivetskiy, P.B. Sigler, C. Schubert, Structure 9 (9) (2001) 869.
[87] J.A. Hirsch, C. Schubert, V.V. Gurevich, P.B. Sigler, Cell 97 (2) (1999) 257.
[88] R.B. Sutton, S.A. Vishnivetskiy, J. Robert, S.M. Hanson, D. Raman, B.E. Knox, M. Kono, J. Navarro, V.V. Gurevich, J. Mol. Biol. 354 (5) (2005) 1069.
[89] B.D. Sachs, G.S. Baillie, J.R. McCall, M.A. Passino, C. Schachtrup, D.A. Wallace, A.J. Dunlop, K.F. MacKenzie, E. Klussmann, M.J. Lynch, S.L. Sikorski, T. Nuriel, I. Tsigelny, J. Zhang, M.D. Houslay, M.V. Chao, K. Akassoglou, J. Cell Biol. 177 (6) (2007) 1119.
[90] H. Murdoch, S. Mackie, D.M. Collins, E.V. Hill, G.B. Bolger, K. Klussmann, D.J. Porteous, J.K. Millar, M.D. Houslay, J. Neurosci. 27 (35) (2007) 9513.